Mirrors with chiral slabs

C. SABAH[*], S. UÇKUN

University of Gaziantep, Electrical and Electronics Engineering Department, 27310, Gaziantep, Turkey

Chiral medium is commonly used in optics, microwave and millimeter-wave due to the possibility of manufacturing chiral materials. Mirrors, considered the most widespread of optical devices, are used for imaging, solar energy collection and in laser cavities. There are two types of mirrors, the well-known metallic ones and the more recent dielectric ones. In this paper, we describe chiral mirror as a structure consisting of an array of alternating chiral layers similar to dielectric mirrors. With this assumption, we construct chiral mirrors of varying parameters and investigate their behaviors for the case of normal incidence.

1. Introduction

Mirrors are known to exist in two types: the well-known metallic ones and the more recent dielectric ones. Imaging, solar energy collection and laser cavities are the most widespread used of mirrors. Metallic mirrors reflect light over a broad range of frequencies incident from arbitrary angles. However, due to a certain amount of absorption, a few percent of the incident power gets lost at infrared and optical frequencies. Multilayer dielectric mirrors, on the other hand, can be extremely low loss but reflect frequencies at a narrow range incident from a particular angular range. Their structure is made of thin layers of materials with different dielectric constants (polystyrene and tellurium) and combines characteristic features of both the metallic and dielectric mirrors. They offer metallic-like omnidirectional reflectivity together with frequency selectivity and low-loss behavior. Fink et. al. [1] discuss dielectric omnidirectional reflectors in their paper. Young and Cristal [2], on the other hand, examine dielectric stacks and present the low-pass and high-pass filter characteristics of the multilayer dielectric stacks.

The electromagnetic features of chiral media are very well known in optics, microwave and millimeter wave communities. Nowadays, due to the progress in the fabrication technologies such materials are employed also in compact integrated components, such as antennas, microwave filters and absorbers, radoms, etc. [3]. Important attention has been focused on the properties of chiral media because the developments in constructing artificial chiral materials provide the additional degree of freedom that these materials offer for design processes via the chirality parameter. Many researchers have studied the interaction of electromagnetic waves with chiral slabs and other possible structures of chiral materials [4–14]. Interaction of electromagnetic waves through multilayer chiral slabs is an important example to these and is discussed by Tanaka and Kusunoki [5]. They computed and presented cross and co-polarized powers and

Stokes parameters of the transmitted and reflected waves for the incident wave of perpendicular polarization. In addition, filter characteristics of periodic chiral layers were investigated by Kalluri and Rao [6] while multilayered chiral filter response at oblique incidence was examined by Cory and Rosenhouse [7]. The subject continues to be of great interest and practical importance owing to a variety of potential applications [10-14]. Among them are absorbers and antireflection coatings.

In this paper, we describe chiral mirror as a structure consisting an array of alternating chiral layers similar to dielectric mirrors. With this assumption, we construct chiral mirrors of varying parameters and investigate their behaviors for the case of normal incidence. Although multilayer chiral structures have been analyzed in the literature [5-7,12], there exists no work which directly relates to chiral mirrors, and this absence has given rise to the present study.

2. Theory

A dielectric mirror (also known as a Bragg reflector) consists of identical alternating layers of high and low refractive indices. The optical thicknesses are typically chosen to be quarter-wavelength long at some operating wavelength λ_0. The standard agreement is to have an odd number of layers, with the high index layer being the first and last layer [15].

A multilayer chiral medium is a combination of layers of N chiral slabs with different material properties and thicknesses [5,7,12]. A chiral mirror is the special case of the multilayer chiral medium, shown in Fig. 1, which is comprised of an array of alternating chiral layers with high and low indices of refraction (n_H and n_L) sandwiched between homogeneous mediums characterized by n_0 (such as air with $n_0 = 1.0$) and n_4. Assuming $\exp(i\omega t)$ time dependence is implicit, the constitutive relations for

the high (low) chiral layer of thickness d_H (d_L) can be defined as follows [4]:

$$D_{H(L)} = \varepsilon_{H(L)} \, E_{H(L)} - j\xi_{cH(cL)} \, B_{H(L)} \qquad (1a)$$

$$H_{H(L)} = -j\xi_{cH(cL)} \, E_{H(L)} + (1/\mu_{H(L)})B_{H(L)} \qquad (1b)$$

where $\varepsilon_{H(L)}$, $\mu_{H(L)}$ and $\xi_{cH(cL)}$ are real constants and state the permittivity, permeability, and chiral admittance of the high (low) chiral layer, respectively.
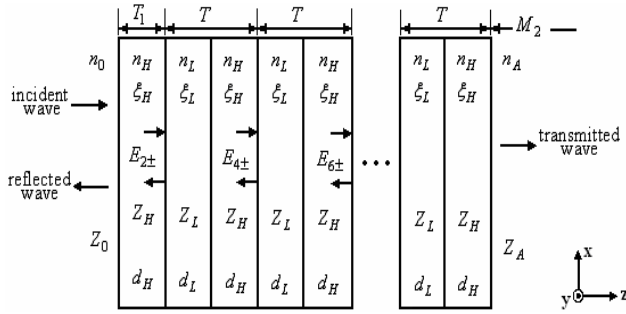
Fig. 1. The structure of chiral mirror.

This provides direct coupling between electric and magnetic fields owing to the chirality of the medium. Note that the quantity $\xi_{cH(cL)}$ indicates the degree of chirality and there is a bound for this quantity given by $\left|\xi_{cH(cL)}\right| \le \sqrt{\varepsilon_{H(L)}/\mu_{H(L)}}$ [3]. A solution to Helmholtz equation in a source free region for the high (low) chiral layer can be expressed as the sum of the left circularly polarized (LCP) and right circularly polarized (RCP) plane waves of different phase velocities. Therefore, there exist four waves in the high (low) chiral layer, two propagating toward the left interface and the other two propagating toward the right interface. The incident field is assumed to be a plane monochromatic wave, which is normally incident upon the multilayer chiral layers from the homogenous medium and it can be written as

$$E_i = [E_{i//}\,a_x + E_{i\perp}\,a_y]\cdot\exp(-jk_0 z) \qquad (2)$$

where a_x and a_y are the unit Cartesian vectors and $k_0 = 2\pi/\lambda_0$ is the free-space wave number. Note that the subscripts $\perp$ and $//$ refer to the perpendicular and parallel components of an electric field vector. In addition, the reflected and transmitted electric fields are denoted by E_r and E_t respectively, and they are expressed in

$$E_r = [E_{r//}\,a_x + E_{r\perp}\,a_y]\cdot\exp(jk_0 z) \qquad (3a)$$

$$E_t = [E_{t//}\,a_x + E_{t\perp}\,a_y]\cdot\exp(-jk_A z) \qquad (3b)$$

where $k_A = 2\pi/\lambda_A$ is the wave number of the transmitted medium. Using the boundary conditions for the fields, the forward-backward fields on one side of the

interface will be related to those on the other side, expressing the relationship in terms of a matching matrix. On account of several interfaces, our forward-backward fields will be propagated from one interface to the next with the help of a propagation matrix. The combination of a matching and a propagation matrix relating the fields across different interfaces will be referred to as a transfer matrix. It is known that to analyze the chiral mirrors shown in Fig. 1 and obtain the matching and propagation matrices, it is necessary to examine in detail the interface between two chiral materials and nonchiral-chiral materials.
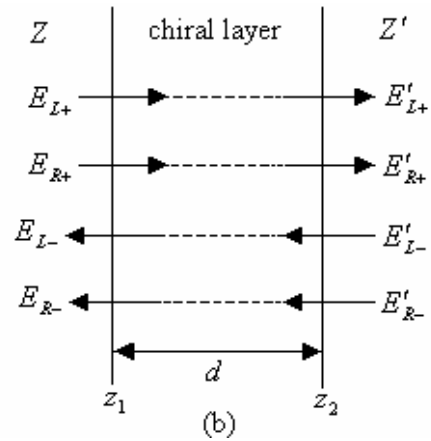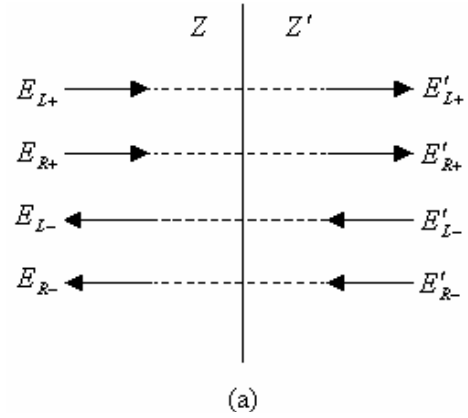
Fig. 2. Electric fields (a) across an interface, (b)propagated through a chiral slab.

We begin by discussing interface of two chiral materials. Consider a planar interface separating two chiral media with characteristic impedances Z and Z', as shown in Fig. 2(a). Because the normally incident fields are tangential to the interface plane, the boundary conditions require that the total electric and magnetic fields be continuous across the two sides of interface. In terms of the x- and y-component of the electric fields, the continuity yields:

$$E_{L+} + E_{R+} - E_{L-} - E_{R-} = E'_{L+} + E'_{R+} - E'_{L-} - E'_{R-} \quad (4a)$$

$$-E_{L+} + E_{R+} - E_{L-} + E_{R-} = -E'_{L+} + E'_{R+} - E'_{L-} + E'_{R-} \quad (4b)$$

Also, the continuity of the magnetic fields gives two equations similar to Equations (4a) and (4b). These contain all the field information at the interface between two chiral media. From this information the matching matrix can be derived which relates the fields on one side of an interface to those of the other side. Because the electric field in a chiral layer is described by four waves (two propagating toward the left interface and the other two propagating toward the right interface), the matching matrix is a 4×4 matrix of the form

$$
\begin{bmatrix} E_{L+} \\ E_{R+} \\ E_{L-} \\ E_{R-} \end{bmatrix} = \begin{bmatrix} \dfrac{(Z/Z')+1}{2} & 0 & 0 & \dfrac{(Z/Z')-1}{2} \\ 0 & \dfrac{(Z/Z')+1}{2} & \dfrac{(Z/Z')-1}{2} & 0 \\ 0 & \dfrac{(Z/Z')-1}{2} & \dfrac{(Z/Z')+1}{2} & 0 \\ \dfrac{(Z/Z')-1}{2} & 0 & 0 & \dfrac{(Z/Z')+1}{2} \end{bmatrix} \begin{bmatrix} E'_{L+} \\ E'_{R+} \\ E'_{L-} \\ E'_{R-} \end{bmatrix} \quad (5a)
$$

or

$$
E = ME' . \quad (5b)
$$

The propagation matrix from location z_1 to location z_2, shown in Fig. 2(b), in a chiral layer is in the form of

$$
P = \begin{bmatrix} \exp(jk_L d) & 0 & 0 & 0 \\ 0 & \exp(jk_R d) & 0 & 0 \\ 0 & 0 & \exp(-jk_L d) & 0 \\ 0 & 0 & 0 & \exp(-jk_L d) \end{bmatrix} \quad (6)
$$

To obtain the matching matrices M_1 and M_2 for the interfaces of nonchiral-chiral materials (first interface of Fig. 1) and the chiral-nonchiral materials (last interface of Fig. 1) the same procedure mentioned above is applied. By setting properly the electric fields and material properties in the left (right) medium of Fig. 2(a) and using the boundary conditions, the matching matrix M_1 (M_2) for the interfaces of the nonchiral-chiral (chiral-nonchiral) materials can be derived.

Now consider the chiral mirror as shown in Fig. 1. If the number of layers is $2N+1$, the number of interfaces will be $2N+2$ and the number of media $2N+3$. After the first layer, we may view the structure as the repetition of N identical bilayers of low and high index. Because the bilayers are identical, the forward-backward fields at the left of one bilayer are related to those at the left of the next one by a transition matrix T, which is product of two matching and two propagation matrices. In this manner, we have

$$
\begin{bmatrix} E_{2L+} \\ E_{2R+} \\ E_{2L-} \\ E_{2R-} \end{bmatrix} = T \begin{bmatrix} E_{4L+} \\ E_{4R+} \\ E_{4L-} \\ E_{4R-} \end{bmatrix} = T^2 \begin{bmatrix} E_{6L+} \\ E_{6R+} \\ E_{6L-} \\ E_{6R-} \end{bmatrix} = T^3 \begin{bmatrix} E_{8L+} \\ E_{8R+} \\ E_{8L-} \\ E_{8R-} \end{bmatrix} = T^4 \begin{bmatrix} E_{10L+} \\ E_{10R+} \\ E_{10L-} \\ E_{10R-} \end{bmatrix} = \dots = T^N \begin{bmatrix} E_{(2N+2)L+} \\ E_{(2N+2)R+} \\ E_{(2N+2)L-} \\ E_{(2N+2)R-} \end{bmatrix} . \quad (7)
$$

Then, the relation between the incident, reflected and transmitted fields can be derived by T_1 and M_2: by an additional transition matrix T_1 we can get to the left of interface-1 and by an additional matching matrix M_2 we pass to the right of the last interface:

$$
\begin{bmatrix} E_{i//} \\ E_{r//} \\ E_{i\perp} \\ E_{r\perp} \end{bmatrix} = T_1 \, T^N M_2 \begin{bmatrix} E_{t//} \\ E_{t\perp} \end{bmatrix} \quad (8)
$$

where $T_1 = M_1 \cdot P_H$, and $T = M_H \cdot P_H \cdot M_L \cdot P_L$. Here M_H (M_L) is the matching matrix that establishes the relation between the fields of high (low) refractive chiral media and low (high) refractive chiral media. Also P_H (P_L) is the propagation matrix of the fields inside the high (low) refractive chiral media. Note that the properties of the chiral mirrors are essentially determined by the Nth power, T^N, of the bilayer transition matrix T. In turn, the behavior of T^N is determined by the eigenvalue structure of T.

3. Numerical results

In this section, above procedure is applied in calculating reflection and transmission responses as a function of the free-space wavelength λ and as a function of frequency $f = c_0 / \lambda$. Incident electric field is assumed to be plane wave with parallel polarization ($E_{i\perp} = 0$). As a first example, we consider the chiral mirror with quarter-wavelength layers and the ratio of chirality parameters is $\xi_{cH}/\xi_{cL} = -1.0$. The high and low indexes are $n_H = 4.20$ and $n_L = 1.46$, corresponding to germanium (Ge) and silicon dioxide (SiO$_2$). The incident medium is air and the transmitted medium is polystyrene with indexes $n_0 = 1.0$ and $n_H = 1.60$. Fig. 3 presents the reflection response for the cases of $2N+1 = 1, 3, 5, 9$ layers. The design wavelength at which the layers are quarter-wavelength long is $\lambda_0 = 3\,\text{cm}$. As the number of layers increase the reflectivity rises and becomes flatter within the bandwidth Δf. Also it has sharper edges and tends to 100%. This is a consequence of the periodic nature of the chiral mirror.
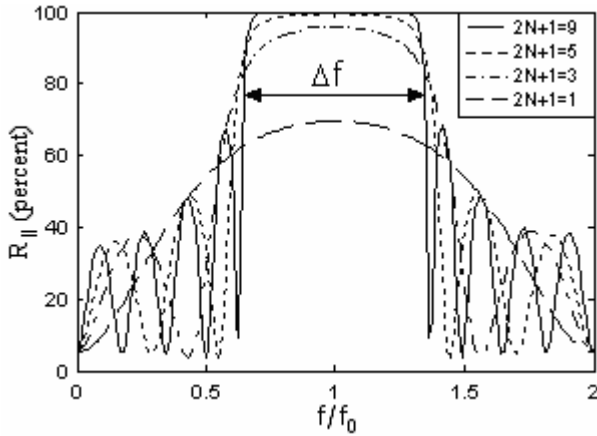
Fig. 3 Reflectivity as a function of f/f$_0$ *for the chiral mirror with quarter-wavelength layers.*
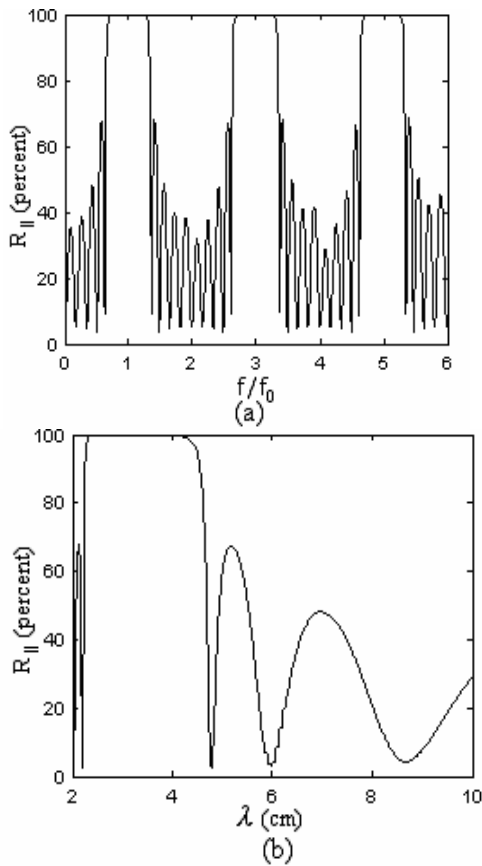
Fig. 4 Reflectivity as a function of f/f$_0$ *and* λ *for the chiral mirror with quarter-wavelength layers.*

In the second example we consider the chiral mirror with quarter-wavelength layers for the case of $N = 4$ bilayers, or $2N + 1 = 9$ layers. The high and low indices and the ratio of chirality parameters are the same with the first example. Fig. 4 shows co-reflectivity as a function of frequency and wavelength. Because the phase thickness of each layer is the same and the matrix T is periodic in the phase thickness, the mirror behavior of the structure

occurs at odd multiples of f$_0$. The maximum reflectivity is equal to 100% at the desired frequency. At this frequency (correspondingly at this wavelength) the parallel and perpendicular component of transmittivity become zero. Note that the cross-reflectivity, $R_\perp$, is zero since the polarization of the reflected wave is the same as that of the incident wave for normal incidence. From Fig. 4(b), the parallel component of reflectivity is 100% at the wide range of the wavelength bandwidth including $\lambda_0 = 3\,\text{cm}$.

In the third example, chiral mirror is considered to be of unequal-length layers. The number of layers and the material properties are the same with the previous one. The length of the layers are $d_H = 0.3\lambda_0/n_H$ and $d_L = 0.2\lambda_0/n_L$. The reflectivity as a function of frequency and wavelength are shown in Fig. 5. The reflectivity is no longer periodic at odd multiples of f$_0$ because the layers do not have equal lengths. In this structure, maximum reflectivity is again, equal to 100%. The bandwidth changes according to the frequency. This can be explained because lengths of the layers are not equal to each other. As a result, it is said that the chiral mirror acts as a Bragg reflector.
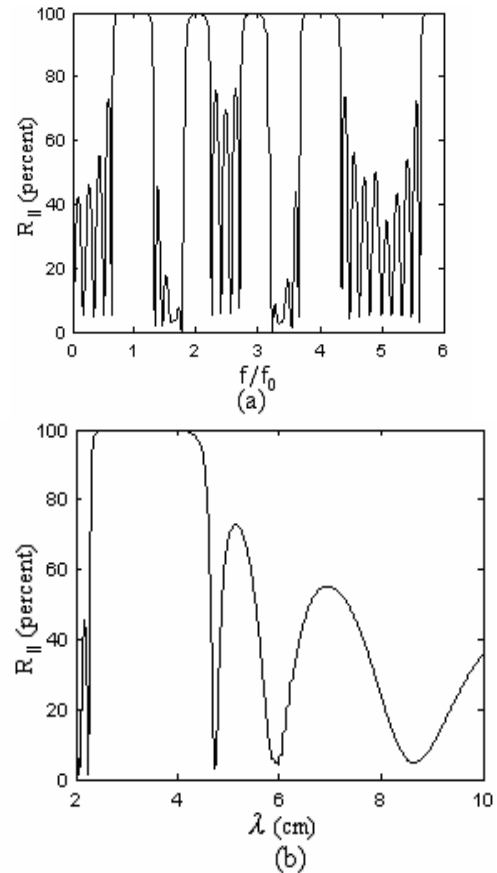
Fig. 5. Reflectivity as a function of f/f$_0$ *and* λ *for the chiral mirror with unequal thicknesses.*
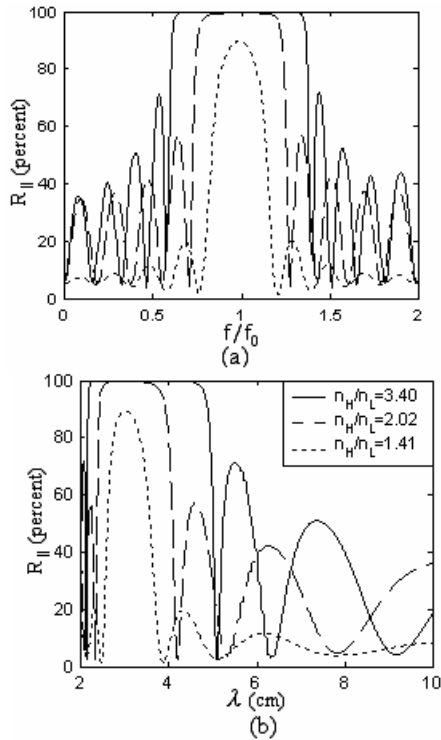
Fig. 6. Reflectivity as a function of f/f_0 and λ for the chiral mirror for the various ratios of refraction indices.
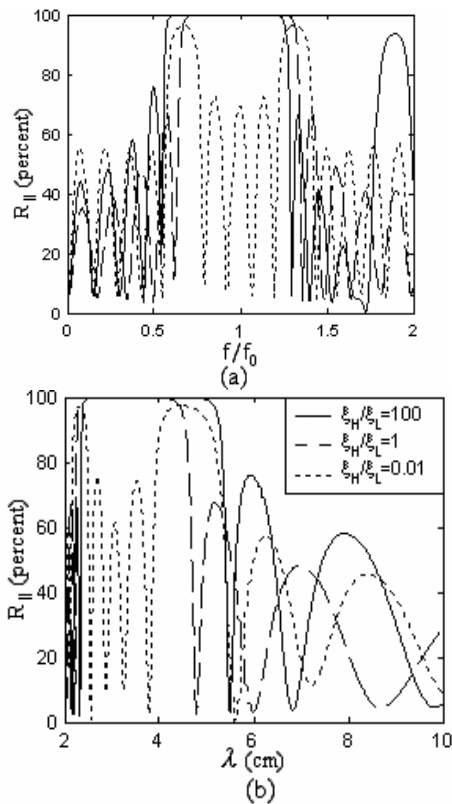
Fig. 7. Reflectivity as a function of f/f_0 and λ for the chiral mirror for the various ratios of chirality parameters.

As a fourth example, the nine-layered chiral mirror with quarter-wavelength layers is considered again.

Numerical results for this structure are presented in Fig. 6 and Fig. 7. Shown in Fig. 6(a) and Fig. 6(b) are reflectivity versus frequency and reflectivity versus wavelength for different ratio of refraction indices when $\xi_{cH}/\xi_{cL} = 1.0$. From these figures, it is easily seen that great ratio indicates high reflectivity (100%) and wide bandwidth, and small ratio indicates low reflectivity and narrow bandwidth. Note that to obtain the ratio for $n_H/n_L = 1.41$ SiO ($n_H = 1.95$) and MgF$_2$ ($n_L = 1.38$), for $n_H/n_L = 2.02$ Si ($n_H = 3.50$) and PbF$_2$ ($n_L = 1.73$), and for $n_H/n_L = 3.40$ Te ($n_H = 4.60$) and Na$_3$AlF$_6$ ($n_L = 1.35$) are used. Fig. 7 illustrates reflectivity as a function of frequency and wavelength for the various ratios of chirality parameters when the high and low indices are the same as the first example. It is seen from Fig. 7(a) that when the ratio is $\xi_{cH}/\xi_{cL} = 0.01$ the reflectivity becomes 70% and the bandwidth is narrow. When the ratio is one or more the reflectivity reaches to 100% and the bandwidth becomes wide. Note that there is no symmetry around the central frequency when the ratio is great (i.e. $\xi_{cH}/\xi_{cL} = 100$). As in Fig. 7(b), when the ratio is decreased (increased) the magnitude of the reflectivity and the bandwidth also decreases (increases). In addition to arranging the ratio n_H/n_L, more efficient (high magnitude reflectivity and wide bandwidth) reflectors can be designed by controlling the chirality parameters. At this point we can say that chiral materials provide the additional degree of freedom for design processes via the chirality parameter.
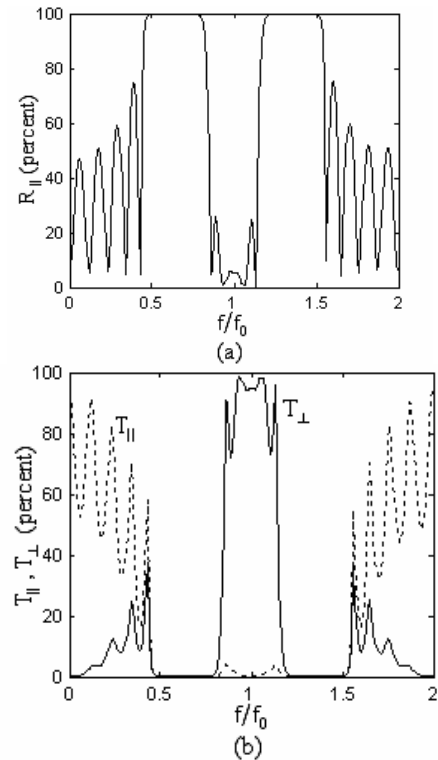
Fig. 8. Reflectivity and transmittivity of the nine-layered chiral mirror as a function of f/f_0 for the thicknesses of the high and low indices half- and quarter-wavelength in length.

As a fifth example, we consider a chiral mirror with nine layers. The high and low indices are selected as germanium ($n_H = 4.20$) and silicon dioxide ($n_L = 1.46$) and the chirality parameters are $\xi_{cH} = \xi_{cL} = 5.2 \times 10^{-4}$ S. The thicknesses of the high and low indices are half- and quarter-wavelength long, respectively. The responses of this structure are demonstrated in Fig. 8 and Fig. 9. The reflectivity and transmittivity versus frequency are presented in Fig. 8. The cross- reflectivity, $R_\perp$, is zero due to the normal incidence.
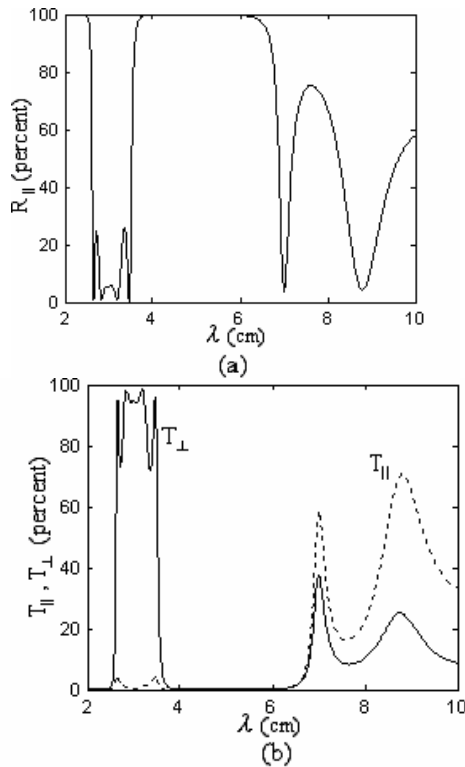
Fig. 9. *Reflectivity and transmittivity as a function of λ for the nine-layered chiral mirror.*

From Fig. 8(a), the co-reflectivity, $R_\parallel$, reaches to 100% between the frequency region $f/f_0 = 0.7$ and $f/f_0 = 1.3$ except $f/f_0 = 1$. Also from Fig. 8(b) the cross-transmittivity, $T_\perp$, reaches to 100% at the $f/f_0 = 1$. At this value a parallel-perpendicular polarization conversion occurs for the transmitted wave. Fig. 9 shows reflectivity and transmittivity as a function of the wavelength. The cross-reflectivity, $R_\perp$, is once again zero due to the normal incidence. The co-reflectivity, $R_\parallel$, and co-transmittivity, $T_\parallel$, are zero at the designed wavelength. Also at this wavelength the cross-transmittivity, $T_\perp$, reaches to almost 100%. It is said that a parallel-perpendicular polarization conversion occurs for

the transmitted wave at the designed wavelength. Therefore, we can say that for the given structure the chiral mirror acts as a polarization-conversion transmission filter. As such, the chiral mirror may also be used as an antireflection filter for the reflected wave.

The same results are obtained as shown in Figs. 3 to 9 for incident wave with perpendicular polarization, i.e., $E_{i\parallel} = 0$.

4. Conclusions

A general analysis of chiral mirrors has been carried out extensively. First of all, the effect of the number of layers to the reflectivity and the bandwidth is discussed. Then the behaviors of the chiral mirror with quarter-wavelength layers and with unequal-length layers are investigated in detail. From these, it is seen that the chiral mirror acts as a Bragg reflector. After that, the effect of the refraction indices and the chirality parameters on reflector properties of the medium is illustrated. From the numerical results, we can say that high magnitude reflectivity and wide bandwidth are not obtained only by arranging the index of refraction of the media, but also by controlling the chirality parameters. Furthermore, chiral materials offer the additional degree of freedom for design processes via the chirality parameter. By using this property more efficient reflectors can be designed. Lastly, the selection of the thicknesses of the high and low index layers determines the filter characteristics of the chiral mirrors. The numerical results demonstrate that the chiral mirrors can be used as an antireflection filter for the reflected wave and as a polarization-conversion transmission filter.

References

[1] Y. Fink, J. N. Winn, S. Fan, C. Chen, J. Michel, J. D. Joannopoulos, E. L. Thomas, A dielectric omnidirectional reflector, Science **282**, 1679 (1998).

[2] L. Young, E. G. Cristal, Low-pass and high-pass filters consisting of multilayer dielectric stacks, IEEE Transactions on Microwave Theory and Techniques **14**, 75 (1966).

[3] N. Engheta, D. L. Jaggard, Electromagnetic chirality and its applications, IEEE Antennas and Propagation Society Newsletter **30**, 6 (1988).

[4] S. Bassiri, C. H. Papas, N. Engheta, Electromagnetic wave propagation through a dielectric-chiral interface and through a chiral slab, Journal of the Optical Society of America A **5**, 1450 (1988).

[5] M. Tanaka, A. Kusunoki, Scattering characteristics of stratified chiral slab, IEICE Transactions on Electronics, vol. E76-C **10**, 1443 (1993).

[6] D. K. Kalluri, T. C. Rao, Filter characteristics of periodic chiral layers, Pure and Applied Optics **3**, 231 (1994).

[7] H. Cory, I. Rosenhouse, Multilayered chiral filter response at oblique incidence, Microwave and Optical Technology Letters **29**, 192 (2001).

[8] M. A. Lyalinov, A. H. Serbest, T. Ikiz, Plane wave diffraction by a thin semi infinite chiral slab, Journal of Electromagnetic Wave Applications **16**, 21 (2002).

[9] K. Delihacioglu, S. Uçkun, Power reflection and transmission coefficients for meander-line polarizers with chiral slab, ETRI Journal **25**, 41 (2003).

[10] F. Bilotti, A. Toscano, L. Vegni, Analysis of cavity antennas with chiral substrates and superstrates though the finite element method, Electromagnetics **24**, 3 (2004).

[11] T. X. Wu, D. L. Jaggard, Scattering of chiral periodic structure, IEEE Transactions on Antennas and Propagation **52**, 1859 (2004).

[12] C. Sabah, S. Uckun, Plane wave reflection and transmission through multilayer chiral slabs, Bianisotropics 2004, Proceedings of the 10th Conference on Complex Media and Metamaterials, Het Pand, Ghent, Belgium, 2004, pp. 29-32.

[13] H. Dakhcha, O. Ouchetto, S. Zouhdi, Chirality effects on metamaterial slabs" Bianisotropic 2004, Proceedings of the 10th Conference on Complex Media and Metamaterials, Het Pand,Ghent, Belgium, 2004, pp. 132-135.

[14] X. Q. Sheny, E. K. N. Yung, Analysis of microstrip antennas on finite chiral substrates, International Journal of RF and Microwave Computer-Aided Engineering **14**, 49 (2004).

[15] S. J. Orfanidis, Electromagnetic Waves and Antennas, On-Line Textbook, Rutgers University, http://www.ece.rutgers.edu/~orfanidi/ewa/

_____
[*]Corresponding author: sabah@gantep.edu.tr